Stress Analysis of Laminated HSDT Beams Considering Bending Extension Coupling

Yonca BAB[1]
Akif KUTLU[2]

ABSTRACT

This study demonstrates a mixed finite element formulation procedure for the bending and stress analyses of laminated composite beams. The finite element method is based on the Hellinger-Reissner variational principle, while the beam assumptions are based on the Higher Order Shear Deformation Theory (HSDT). Reddy's shear function is employed for the beam theory where the beam is discretized by two-noded linear elements. The displacements and stress resultants are obtained directly at the nodes according to the proposed mixed formulation. The validation of current study is performed by comparison and convergence analyzes for various lamination cases under different boundary conditions.

Keywords: Higher Order theory, laminated composite beam, Hellinger-Reissner, mixed finite element formulation, stress analysis.

1. INTRODUCTION

Nowadays, composite structures are frequently used in engineering fields such as construction, machinery, biomechanics, nuclear, automotive, aerospace and defense industries [1]. These composite materials, based on the physical properties of the different materials, provide advantages such as heat, sound and water insulation, fire safety, high resistance, corrosion resistance, low cost and low weight in the structures they are integrated. Accurate prediction of bearing capacity, failure load, and damage conditions are critical in the structural design of composite materials to be more efficient as intended. In this context, the need for detailed and accurate static analysis of composite structures is inevitable. Since the financial situation or the physical environment is not always suitable for experimental works, it is much more efficient to employ numerical analyses with possibly most realistic reflection of the mechanical behavior depending on the problem type. Although elasticity based analytical solutions may provide exact behavior of structural elements, the application

of such an approach is limited to certain types of boundary conditions, loading case and geometries [2]. In the literature, different theories have been put forward to perform static or dynamic analyses of beam type structures. Classical Theory (CT), First-Order Shear Deformation Theory (FSDT), Higher-Order Shear Deformation Theory (HSDT) and Zigzag Theories (ZZT) [3,4] are among the leading theories. CT, also known as Bernoulli-Euler theory, was proposed by Euler [5] and Bernoulli [6] about 280 years ago and provides good enough predictions of mechanical behavior when the beam is thin. Boley [7] can be given as an example of the early usage of CT, and Modaress-Aval et al. [8] can be given as an example of the resent usage of this theory. FSDT, developed by Timoshenko [9] and also named after him, takes into account rotational inertia and first-order shear effects. Some examples of studies that analyzed composite beams with FSDT can be cited as Wagner and Gruttman [10] and Lee and Jang [11]. On the other hand, HSDT can describe along-thickness transverse deformations so that taking cross-sectional distortion into account by introducing higher-order shear terms in the forms of polynomial-based, trigonometric, and exponential functions etc. Researchers working on beam-plate theories include Reddy [12], Reissner [13], Soldatos [14] who have derived and tested various shear terms in their formulations. Ferreira et al. [15], Murthy et al. [16] and Madenci [17] analyzed composite beams with HSDT. Chandrashekhara and Bangera [18] investigated the free vibration behavior of laminated composite beams by using HSDT, including the effect of Poisson ratio, which is generally neglected in one-dimensional models. Maiti and Sinha [19] have developed a finite element (FE) model based on HSDT, that takes into account the deformations in the thickness direction while examining the bending and free vibration behavior of laminated composite beams. Xiaoping and Liangxin [20] introduced a third-order shear deformation theory that ensures the continuity of in-plane displacements and transverse shear stresses between adjacent layers. Meanwhile, the representation of the displacement variables is similar to the FSDT. While focusing on the bending behavior of cross-layered composite and sandwich beams, Zenkour [21] used the HSDT and included the deformation in the thickness direction into the calculations. Matsunaga [22] studied the natural frequency and buckling behavior of laminated composite beams subjected to axial stress by benefiting from the one-dimensional HSDT and Hamilton's principle. Here, the transverse shear assumption takes into account the full effects of normal stress in the thickness direction as well as rotational inertia. Subramanian [23] carried out a free vibration analysis of laminated composite beams based on finite element method (FEM) with two different HSDTs that take into account the deformation in the beam thickness direction. In these two theories, there are five and four variations of the in-plane and transverse displacements through the thickness coordinates of the beams, respectively, and zero transverse shear stress conditions on the upper and lower surfaces of the beams are satisfied. Zhen and Wanji [24] examined the static and dynamic behavior of sandwich and laminated composite beams using displacement-based HSDT. Ozutok and Madenci [25] combined mixed finite element method (MFEM) and HSDT to perform static analysis of laminated composite beams. Kutlu et al. [26–28] and Aribas et al. [29–31] revealed some advantages of MFEM based formulations on the prediction of accurate stress resultants and stress components of various beam, helix and plate type structures. Shao et al. [32] proposed a new HSDT for the free vibration analysis of laminated composite beams. Based on the kinematic assumptions of this theory, bending and transverse shear strains are independent from each other, such that the beam deflection is defined as the resultant of bending and shear related terms. A generalized approach is presented to satisfy the condition of zero shear stress on the lower and upper free surfaces of the beam. Sayyad

and Ghugal [33] compiled studies that performed bending, buckling and free vibration analysis of laminated composite and sandwich beams in their literature review article.

When the literature is examined, it can be seen that CT, which ignores the shear effects, and FSDT, which needs a shear correction coefficient, are insufficient in solving relatively thick elements used in composite construction. For this reason, in this study, HSDT is used in the mechanical model of laminated composite beams and the shear function proposed by Reddy is employed. By introducing an efficient mixed finite element formulation, it is aimed to provide accurate determination of stress components alongside displacement terms. In this regard, this study extends the idea presented in Bab and Kutlu [34] by adding axial displacement into kinematic field. Thus, bending-extension coupling effect can be considered in the analyses. The Hellinger-Reissner principle was used to describe the energy expression of the laminated composite beam in linear elastic regime. In the displacement field, one axial displacement, one deflection and one rotation term are assigned. The corresponding finite element functional is of a mixed form and involves stress resultant terms besides displacement components. In generating the system finite element equations, two-noded elements are described with linear shape functions, and integrals of energy expressions are calculated numerically over a two-point Gauss quadrature scheme. By solving the finite element equations, the bending moment, higher order bending moment and the shear force, alongside the axial displacement, deflection and rotation components, are obtained directly at the nodal points. This way, strain measures can be calculated using sectional compliance matrices without using derivatives, thus the accuracy of the axial stress calculation compared to displacement-based finite elements is improved satisfactorily. Transverse shear stresses are obtained along the thickness of the laminated beam by placing the calculated axial stresses in the equilibrium equations presented by the theory of elasticity. By increasing the number of elements in the beam domain some convergence analyses were carried out with repeated solutions, and comparison analyzes were carried out considering the elasticity solutions in the literature and various numerical procedures. Afterwards, solutions are presented in which various layout, loading, and boundary conditions are taken into account to demonstrate the effectiveness of the proposed finite element formulation in the displacement and stress calculation of laminated composite beams. Also, the influence of the bending-extension coupling in nonsymmetrically laminated beams with axially constrained end conditions is examined.

2. FIELD EQUATIONS AND NUMERICAL FORMULATION

Consider the beam in Figure 1a, loaded in its x, z plane, where x describes the beam axis and the cross-section lies within the y, z plane. The kinematic field of the beam under the distributed load acting in the z-direction along the beam axis can be described according to the HSDT as follows:

$$u^* = u - z\, w,_x + f(z)\theta_x$$
$$w^* = w \tag{1}$$

Here, $u^*(x,z)$ and $w^*(x,z)$ denote axial and transverse displacement field of the beam, respectively, whereas $u(x)$ is the axial displacement and $w(x)$ is the deflection of the beam at its centroid. Also, $\theta_x(x)$ describes the rotation of the section about the y-axis. In addition, $f(z)$ is the shear function defined to reflect the distortion of the section. In the current study, Reddy's [35] shear function is employed:

$$f(z) = z\left(1 - \frac{4z^2}{3h^2}\right) \tag{2}$$

In this expression, h denotes the height of the beam (See Figure 1b). The strain components along the beam section are written over the displacement field described in equation (1) as follows:

$$\varepsilon_{xx} = u,_x^* = u,_x - z\,w,_{xx} + f\theta_{x,x}$$
$$\gamma_{xz} = u,_z^* + w,_x^* = f'\theta_x \tag{3}$$

The commas in the subscript indicates that the derivatives are taken according to the axis variables that follow it. In Equation (3), the strain measures can be denoted as follows:

$$\begin{Bmatrix} \varepsilon_m \\ \kappa_0 \\ \kappa_1 \\ \varepsilon_s \end{Bmatrix} = \begin{Bmatrix} u,_x \\ -w,_{xx} \\ \theta_{x,x} \\ \theta_x \end{Bmatrix} \tag{4}$$

(a)   (b)   (c)
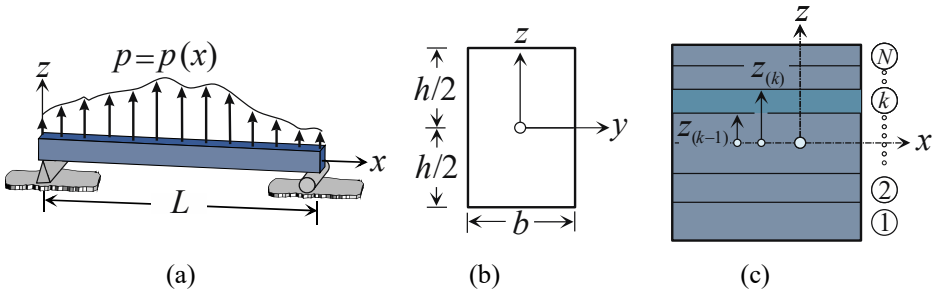
Figure 1 - Laminated composite beam a) Beam axis b) Beam cross-section and dimensions c) Lamination

The stress-strain relationships in any k'th layer of the composite beam shown in Figure 1c can be written by using Hooke's law in the form:

$$\left\{\begin{matrix} \sigma_{xx} \\ \sigma_{xz} \end{matrix}\right\}^{(k)} = \begin{bmatrix} \bar{Q}_{11} & 0 \\ 0 & \bar{Q}_{55} \end{bmatrix}^{(k)} \left\{\begin{matrix} \varepsilon_{xx} \\ \gamma_{xz} \end{matrix}\right\}^{(k)} \tag{5}$$

Here, $\bar{Q}_{11}$ and $\bar{Q}_{55}$ correspond to the transformed material stiffness terms of the orthotropic material in the k'th layer to the global axis of the beam [36]. $\sigma_{xx}^{(k)}$ and $\sigma_{xz}^{(k)}$ are axial normal stress and transverse shear stress components in the layer. The first variation of the functional of an elastic system can be stated according to the Hellinger-Reissner principle as follows [37,38].

$$\delta\Pi_{HR} = \int_V \left(\boldsymbol{\varepsilon}^{\mathbf{u}} - \boldsymbol{\varepsilon}^{\boldsymbol{\sigma}}\right)^T \delta\boldsymbol{\sigma}^{\boldsymbol{\sigma}} dV + \int_V \left(\left(\boldsymbol{\sigma}^{\boldsymbol{\sigma}}\right)^T \delta\boldsymbol{\varepsilon}^{\mathbf{u}} - \mathbf{q}^T \delta\mathbf{u}\right) dV - \int_\Gamma \hat{\mathbf{t}}^T \delta\mathbf{u} d\Gamma = 0 \tag{6}$$

In this equation, the first integral corresponds to the weak form of the compatibility conditions of the strain ($\boldsymbol{\varepsilon}$) field, while the second integral corresponds to the weak form of the equilibrium equations in the volume (V) domain under the influence of external load $\mathbf{q}$. In the first integral, the compatibility between the description of the strain field ($\boldsymbol{\varepsilon}^{\mathbf{u}}$) over the kinematic relations and the description ($\boldsymbol{\varepsilon}^{\boldsymbol{\sigma}}$) over the stresses is determined. The last integral shows the work done by the stresses $\hat{\mathbf{t}}^T$ at the boundary of the region Γ . Here δ is the variation operator. When the equation (6) given for the general three-dimensional case is to be reduced to the beam problem, the integrals of the stress components along the thickness are calculated and instead of stress and strain components, stress resultants and strain measures are placed:

$$\delta\Pi_{HR} = \int_L \left(\mathbf{e}^{\mathbf{u}} - \mathbf{e}^{\mathbf{P}}\right)^T \delta\mathbf{P} dL + \int_L \left(\mathbf{P}^T \delta\mathbf{e}^{\mathbf{u}} - \mathbf{p}^T \delta\mathbf{u}\right) dL - \int_\Gamma \hat{\mathbf{t}}^T \delta\mathbf{u} d\Gamma = 0 \tag{7}$$

Here, $\mathbf{e}^{\mathbf{u}} = [\varepsilon_m \quad \kappa_0 \quad \kappa_1 \quad \varepsilon_s]^T$ is strain measures vector expressed over kinematic relations while $\mathbf{e}^{\mathbf{P}}$ collects strain measures in terms of stress resultants. $\mathbf{P}^T = [N_{xx} \quad M_{xx} \quad M_{xx}^f \quad Q_{xz}]$ is stress resultants vector and $\mathbf{p}$ denotes transversely applied load acting along the beam. The expression of axial force N_{xx}, bending moment M_{xx}, higher order bending moment M_{xx}^f and shear force Q_{xz} in terms of stress components is as follows:

$$\left(N_{xx}, M_{xx}, M_{xx}^f, Q_{xz}\right) = b\sum_{k=1}^N \int_{z_{(k-1)}}^{z_{(k)}} \left(\sigma_{xx}^{(k)}, z\sigma_{xx}^{(k)}, f(z)\sigma_{xx}^{(k)}, (df(z)/dz)\sigma_{xz}^{(k)}\right) dz \tag{8}$$

Here, b is the beam width (see Figure 1b) and N is the total number of layers in the section. When the constitutive relations given in Equation (5) are placed in Equation (8), the relationship between strain measures $\mathbf{e}^{\mathbf{u}}$ and stress resultants $\mathbf{P}$ is found as follows:

$$
\mathbf{P} = \mathbf{Ee}^{\mathbf{u}} \quad \text{or} \quad
\begin{Bmatrix} N_{xx} \\ M_{xx} \\ M_{xx}^f \\ Q_{xz} \end{Bmatrix} =
\begin{bmatrix}
A_{11} & B_{11} & E_{11} & 0 \\
B_{11} & D_{11} & F_{11} & 0 \\
E_{11} & F_{11} & H_{11} & 0 \\
0 & 0 & 0 & A^s
\end{bmatrix}
\begin{Bmatrix} \varepsilon_m \\ \kappa_0 \\ \kappa_1 \\ \varepsilon_s \end{Bmatrix}
\tag{9}
$$

Here, the terms of the sectional stiffness matrix $\mathbf{E}$ are calculated as follows:

$$
\left(A_{11} \quad B_{11} \quad D_{11} \right) = b \sum_{k=1}^{N} \int_{z_{(k-1)}}^{z_{(k)}} \overline{Q}_{11}^{(k)} \left(1 \quad z \quad z^2 \right) dz
$$

$$
\left(E_{11} \quad F_{11} \quad H_{11} \right) = b \sum_{k=1}^{N} \int_{z_{(k-1)}}^{z_{(k)}} \overline{Q}_{11}^{(k)} \left(f(z) \quad zf(z) \quad f(z)^2 \right) dz
\tag{10}
$$

$$
A^s = b \sum_{k=1}^{N} \int_{z_{(k-1)}}^{z_{(k)}} \overline{Q}_{55}^{(k)} \left(f'(z) \right)^2 dz
\tag{11}
$$

If equation (9) is arranged for use in equation (7) by describing the compliance matrix $\mathbf{S} = \mathbf{E}^{-1}$, the new form is obtained as:

$$
\mathbf{e}^{\mathbf{P}} = \mathbf{SP} \quad \text{or} \quad
\begin{Bmatrix} \varepsilon_m \\ \kappa_0 \\ \kappa_1 \\ \varepsilon_s \end{Bmatrix} =
\begin{bmatrix}
A'_{11} & B'_{11} & E'_{11} & 0 \\
B'_{11} & D'_{11} & F'_{11} & 0 \\
E'_{11} & F'_{11} & H'_{11} & 0 \\
0 & 0 & 0 & A'^s
\end{bmatrix}
\begin{Bmatrix} N_{xx} \\ M_{xx} \\ M_{xx}^f \\ Q_{xz} \end{Bmatrix}
\tag{12}
$$

Equilibrium equations of the laminated composite beam, in which higher order shear effects are taken into account, are given as follows:

$$
\left.
\begin{aligned}
N_{xx,x} &= 0 \\
p + M_{xx,xx} &= 0 \\
M_{xx,x}^f - Q_{xz} &= 0
\end{aligned}
\right\}
\tag{13}
$$

Finally, using equations (13), (12) and (4) in equation (7), the first variation of the functional of the laminated composite beam becomes:

$$\delta\Pi_{HR} = \int_L \left[w_{,x} \delta M_{xx,x} - \left(\bar{D}_{11} M_{xx} + \bar{F}_{11} M_{xx}^f \right) \delta M_{xx} \right] \mathrm{d}L$$

$$+ \int_L \left[\theta_{x,x} - \left(\bar{F}_{11} M_{xx} + \bar{H}_{11} M_{xx}^f \right) \right] \delta M_{xx}^f \mathrm{d}L + \int_L \left[\theta_x - \left(\bar{A}^s Q_{xz} \right) \right] \delta Q_{xz} \mathrm{d}L \tag{14}$$

$$- \int_L \delta w p \, \mathrm{d}L + \int_L \left(M_{xx,x} \, \delta w_{,x} + M_{xx}^f \delta \theta_{x,x} + V_{xz} \delta \theta_x \right) \mathrm{d}L - \int_\Gamma \hat{\mathbf{t}}^T \delta \mathbf{u} \, \mathrm{d}\Gamma = 0$$

In Equation (14), L represents the beam length and Γ represents the beam boundary. This equation contains both displacement and force-force couple type field variables. In the expression of the first variation of the functional given by Equation (14), the second order derivatives on the terms are reduced to the first order using partial integration, as an advantage of the mixed finite element formulation. In this way, it is ensured that the shape functions to be used in the finite element discretization to be created have C_0 continuity. The generated two-node linear shape functions (Figure 2a) for any coordinate ξ in the interval $-1 \le \xi \le 1$ (Figure 2b) can be expressed as:

$$\varphi_i(\xi) = \tfrac{1}{2} \left(1 + \xi \xi_i \right), \quad i = 1, 2 \tag{15}$$

When equation (14) is discretized with the introduced two-noded linear elements, the finite element equations are obtained in the following form:

n_d : node number
n_e : element number

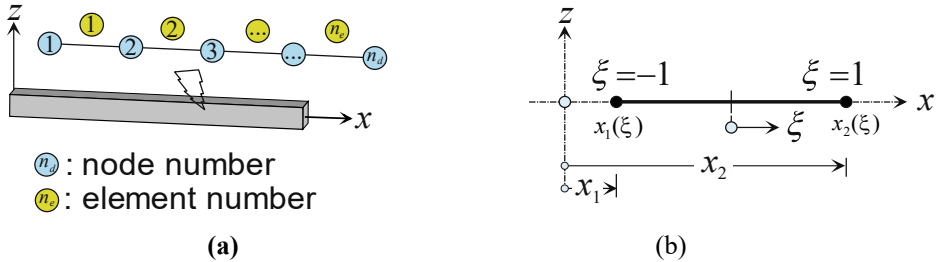**(a)**   (b)

Figure 2 - Finite element definition a) Linear two-noded element discretization in beam domain, b) Global and local coordinate systems in a general element

$$\mathbf{KX} = \mathbf{F} \tag{16}$$

In Equation (16), $\mathbf{K}$ corresponds to the system matrix, $\mathbf{F}$ corresponds to the external force vector, and $\mathbf{X}$, whose expansion is given for any node (i) in Equation (17), corresponds to the unknowns vector.

$$\mathbf{X}^i = \begin{bmatrix} u^i & w^i & \theta_x^i & N_{xx}^i & M_{xx}^i & M_{xx}^{fi} & Q_{xz}^i \end{bmatrix}^T \tag{17}$$

By solving Equation (16), both the displacement type and the stress resultant type field variables for the laminated composite beam are obtained directly at the nodal points. In this

way, strain measures can be calculated directly by matrix operations using Equation (12) without requiring any numerical derivative operations. Then, by using kinematic and constitutive relations, the distribution of stress components along the cross-section can be obtained again at the nodal points. However, due to the assumptions of higher order shear deformation theory the calculation of transverse shear stresses with the help of constitutive relations can produce unrealistic results. If the equilibrium equations of the theory of elasticity are used to overcome this problem, the transverse shear stress component can be determined at any thickness coordinate as follows:

$$\sigma_{xz} = -\int_{-h}^{\bar{z}} (\partial \sigma_{xx} / \partial x) \mathrm{d}\bar{z} \tag{18}$$

3. NUMERICAL RESULTS

A number of numerical examples have been studied in order to show the performance and efficiency of the proposed mixed finite element formulation in stress and displacement calculation under static loading for laminated composite beams and the results are interpreted. The solutions are obtained through a Fortran-based program developed by the authors. Firstly, the convergence behavior of the numerical solution method was examined and by making comparisons with 3D elasticity solution of Pagano [39] which is accepted as a reference solution in the literature; the accuracy of the formulation and the developed program has been tested. Afterwards, solutions were presented for various lamination, loading and support conditions, and the effectiveness of the formulation was investigated by comparing its results with studies such as Hasim (isogeometric zigzag formulation) [40], Vidal and Polit [41] (sinusoidal zigzag), Khdeir and Reddy [42] (analytical solution of higher order theory), Kapuria et al. [43] (zigzag) and Zenkour [21] (simple higher order theory). In the presented problems, common engineering material constants are defined as follows:

Material 1: $E_1 / E_2 = 25, G_{12} = G_{13} = 0.5E_2, G_{23} = 0.2E_2, \nu_{12} = \nu_{23} = 0.25$

Material 2: $\left(E_1 = 181, E_2 = 10.3, G_{12} = G_{13} = 7.17, G_{23} = 2.87\right)$[GPa]

$\nu_{12} = 0.25, \nu_{23} = 0.33$

Here, E_1 and E_2 are Young's moduli of orthotropic material in material principal directions. G_{ij}, $((i,j) = 1,2,3)$ stands for the shear moduli and υ_{ij}, $((i,j) = 1,2,3)$ represents Poisson's ratio. Material 2 is employed for the comparison study of Kapuria et al. [43] (see Table 3). The rest of the examples and comparison studies are performed according to the Material 1 properties.

3.1. Symmetric - Antisymmetric Laminated Beam under Sinusoidal Load

The solution of the one end simple supported and the other end is sliding symmetric and antisymmetric laminated beam using the proposed mixed finite element formulation has been compared with the literature. The beam is under the effect of a distributed transverse

sinusoidal load $p(x) = p_0 \sin(\pi x/L)$ along its axis. The cross section layouts [0/90] and [0/90/0] are described with material lamination angles and each layer of equal thickness is considered to be formed with Material 1. The antisymmetrically laminated beam is also compared with simply supported but not sliding (fixed axial displacement) boundary conditions. $\rho = L/h = 4, 20, 40$ values were taken as the beam span to thickness ratio, and solutions were obtained by using the number of elements $n_e = 10, 20, 30, 40$ along the beam to observe the convergence behavior of the results of deflection and stress components. In order to evaluate the results presented in Table 1 in general way, the following non-dimensionalization procedures have been carried out:

$$\bar{w} = \frac{10^2 E_2 h^3 b w(L/2, 0)}{p_0 L^4} \quad , \quad \bar{\sigma}_{xx} = \tfrac{b}{p_0} \sigma_{xx}(L/2, -h/2)$$
$$(\bar{\sigma}_{xz}^a, \bar{\sigma}_{xz}^b) = \tfrac{b}{p_0}\left(\sigma_{xz}(0,0) \ , \ \sigma_{xz}(0, -h/4) \right) \tag{19}$$

Table 1 - Symmetric and antisymmetric simply supported laminated composite beam (one end is sliding) under sinusoidal loading

Layups	Theory	$\rho = 4$			$\rho = 20$			$\rho = 40$		
		$\bar{w}$	$\bar{\sigma}_{xx}$	$\bar{\sigma}_{xz}$	$\bar{w}$	$\bar{\sigma}_{xx}$	$\bar{\sigma}_{xz}$	$\bar{w}$	$\bar{\sigma}_{xx}$	$\bar{\sigma}_{xz}$
	MHBT ($n_e = 10$)	2.656	-16.850	1.521	0.593	-257.232	8.586	0.525	-1007.5	17.237
	MHBT ($n_e = 20$)	2.689	-16.955	1.549	0.600	-258.822	8.747	0.532	-1013.7	17.560
[0/90/0][a]	MHBT ($n_e = 30$)	2.695	-16.974	1.554	0.601	-259.119	8.777	0.533	-1014.8	17.620
	MHBT ($n_e = 40$)	2.697	-16.981	1.556	0.602	-259.222	8.788	0.533	-1015.3	17.641
	Hasim	2.804	-15.9	1.44	0.6134	-258.9	8.681	0.5362	-1015.3	17.563
	Vidal and Polit	2.803	-19.5	1.42	0.6151	-265.4	8.699	0.5371	-1024.4	17.540
	Pagano (Exact)	2.8899	-18.8	1.432	0.618	-263.2	8.748	0.5379	-1019.7	17.761
	MHBT ($n_e = 10$)	4.3779	-33.3	2.908	2.6556	-697.7	14.327	2.6007	-2773.5	28.641
	MHBT ($n_e = 20$)	4.4324	-33.5	2.962	2.6885	-702.0	14.595	2.6329	-2790.6	29.177
[0/90][b]	MHBT ($n_e = 30$)	4.4425	-33.6	2.973	2.6946	-702.8	14.646	2.6389	-2793.8	29.277
	MHBT ($n_e = 40$)	4.4461	-33.6	2.976	2.6968	-703.1	14.663	2.6410	-2795.0	29.313
	Hasim	4.5175	-26.8	2.871	2.6996	-692.5	14.644	2.6419	-2788.1	29.372
	Vidal and Polit	4.5438	-31.8	2.843	2.7036	-703.6	14.574	2.6450	-2803.1	29.174
	Pagano (Exact)	4.7076	-30	2.706	2.7092	-699.7	14.62	2.6462	-2793.0	29.325

In the Table 1, MHBT (Mixed Higher Order Beam Theory) represents the present theory of this study. As it can be followed from Table 1, the proposed numerical solution method exhibits a stable convergence behavior. A case of converging values for both displacement and stress components from below (growing with increasing number of elements) is observed. In the case of very thick beams, it can be seen that the displacement results are noticeably different from the elasticity results, which is a natural consequence of the higher order shear deformation theory. Nevertheless, it has been observed that the stress values obtained in this study for the symmetrical laminated case fit the elasticity solution with a

much better approximation (except $\bar{\sigma}_{xz}$ value for $\rho = 4$) compared to the rather advanced lamination theories and solution methods. This case is valid for all thicknesses of the laminated beam. Although the antisymmetric lamination is a challenging situation, the presented numerical solution procedure can produce very realistic results. To give an example for the convergence values, regarding the comparison made with the elasticity solution for $\rho = 40$ in the Table 1 and the finest element mesh (40 elements), it has been observed that the normal stress of the symmetrical structure has a difference of 0.43%, while the antisymmetric structure has a difference of 0.07%.
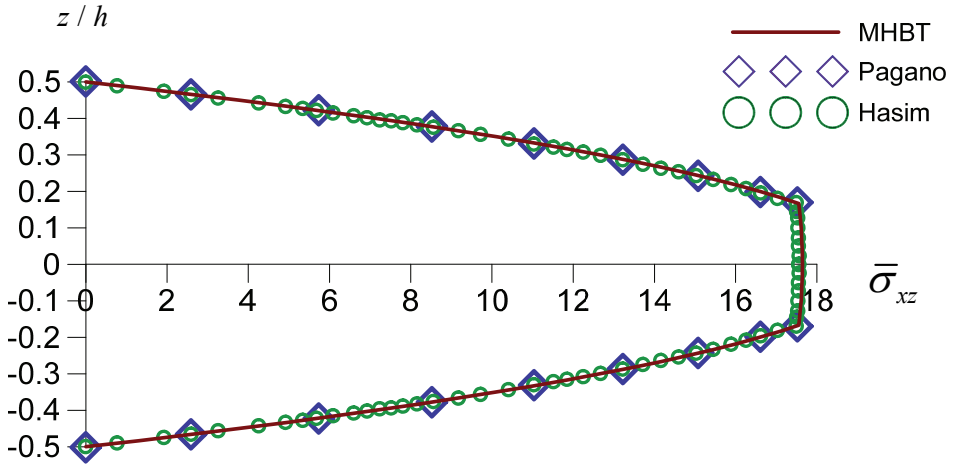
Figure 3 - Transverse shear stress distribution in a sinusoidal loaded, simply supported laminated composite beam (Material 1)
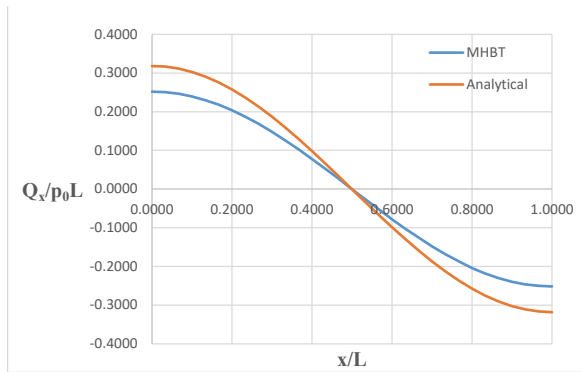

Figure 4 - Shear force distribution in a sinusoidally loaded, simply supported laminated composite beam (Material 1)

Figure 3 shows the shear stress distribution in the thickness direction of the sinusoidally loaded laminated composite beam with [0/90/0] layout scheme. Solution was made for $\rho = 40$ ratio employing 40 elements. The results of MHBT are also compared with the solutions offered by Pagano [39] ve Hasim [40]. As can be seen in the figure, it was observed that the transverse shear stress values obtained from all three solutions overlapped one another.

In Figure 4, the comparison between the shear force calculated by the proposed numerical method and the shear force obtained by using the classical equilibrium equations of the composite beam with sinusoidal load and simple support is given. Due to the assumptions of the higher order beam theory, shear force establishes an equilibrium state with higher order moments. Therefore, the shear force obtained directly from the finite element solution as the field variable is not equal to the resultant of the (real) transverse shear stress that is distributed in the cross section. If it is desired to calculate more realistic shear force values within the framework of a higher order shear theory, integrals of shear stresses along the cross-section obtained by using the equilibrium equations of the elasticity theory can be evaluated.

In Figure 5, the moment distribution of the analytical solution for the symmetrically laminated composite beam under sinusoidal loading is compared with the distribution obtained by the mixed finite element method and it has been observed that the proposed finite element method perfectly reflects the equilibrium equations.
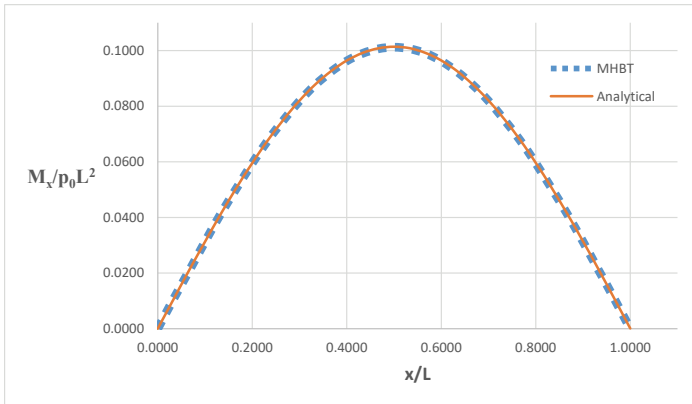

Figure 5 - Bending moment distribution in a sinusoidally loaded, simply supported laminated composite beam with $\rho = 20$ ratio (Material 1)

In Figure 6, deflection (nondimensionalized according to Equation (19)) variations along the beam length for simply-simply supported and simply-sliding supported conditions under sinusoidal loading are presented. For the simply-sliding case, the maximum deflection value is 1.93 times larger than the simply-simply case. The reason of this difference is that for simply-simply supported case, the extension bending coupling effect takes place so the deflections of the beam reduce when compared to sliding case.

In Figure 7, moment distribution along the beam length for simply-simply supported and simply-sliding supported conditions can be observed. As can be seen from the figure, moment distribution overlaps in both boundary conditions.
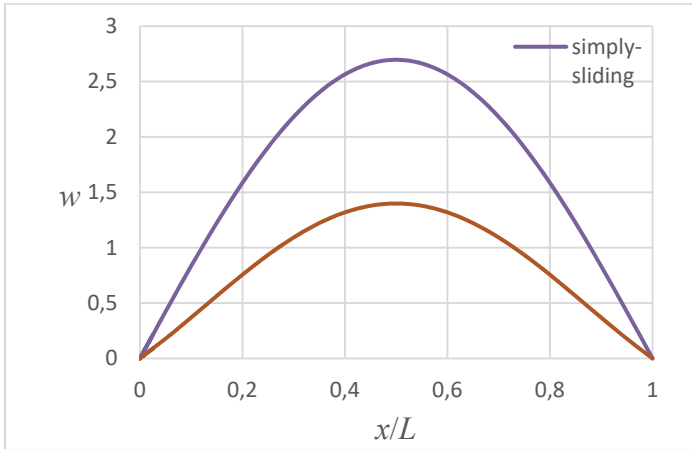

Figure 6 - Deflection (dimensionless) along the beam axis for antisymmetric [0/90] laminated composite beam with $\rho = 20$ ratio
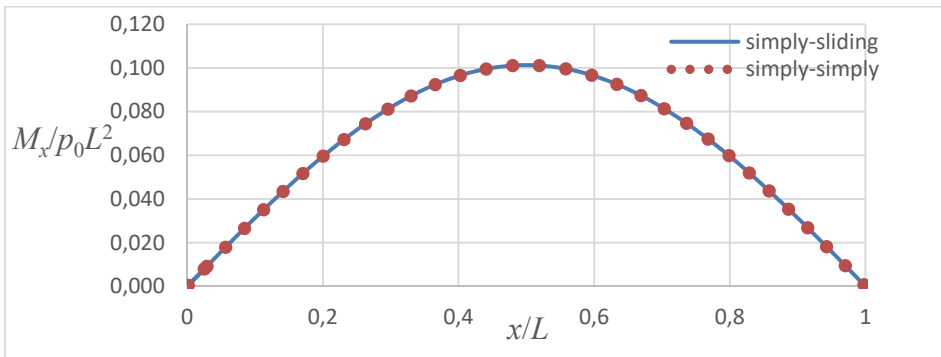

Figure 7 - Moment distribution along the beam axis for antisymmetric [0/90] laminated composite beam with $\rho = 20$ ratio under sinusoidal loading

3.2. Various Laminated Beams under Uniform Load

Uniformly $p(x) = p_0$ loaded beams with [0/90], [0/90/0] and [0/90/90/0] lamination layouts are discussed in this section. While the simple support condition is considered for all lamination layouts, only the layout of [0/90/0] is taken into account in the clamped support condition. In Table 2, the mid-span deflection values of the clamped beam made of Material 1 are presented for various thickness to span ratios and number of elements. The predictions of MHBT are also compared with the analytical solution provided by Khdeir and Reddy [42]

for the higher-order beam theory. When Table 2 is examined, it can be stated that the proposed solution method shows a consistent convergence behavior also under the clamped boundary condition. It can be said that mixed finite element results are in good agreement with the analytical results for all thickness ratios. Another important result that can be extracted from the Table 2 is that with the increase of the beam span-thickness ratio, the deflection values demonstrate a faster convergence regarding the mesh refinement.

Table 2 - Symmetric laminated composite beam under uniform loading

		$\bar{w}$		
Layup	Theory	$\rho = 5$	$\rho = 10$	$\rho = 50$
	MHBT $(n_e = 10)$	1.5081	0.5130	0.1456
	MHBT $(n_e = 20)$	1.5351	0.5286	0.1466
[0/90/0]	MHBT $(n_e = 30)$	1.5371	0.5310	0.1469
	MHBT $(n_e = 40)$	1.5376	0.5316	0.1471
	Khdeir and Reddy	1.537	0.532	0.147

In Table 3, the comparison of the displacement and stress components of a uniformly loaded composite simply supported beam having a symmetrical [0/90/90/0] layout with the elasticity solution and a third order theory solution is made. Nondimensional parameters in this table are calculated according to the following expressions,

$$
\bar{w} = \frac{10^2 E_2 h^3 b}{p_0 L^4} w(L/2, 0) \quad , \quad \bar{\sigma}_{xx} = \frac{h^2 b}{p_0 L^2} \sigma_{xx}(L/2, h/2) \quad ,
$$
$$
\bar{\sigma}_{xx}^* = \frac{h^2 b}{p_0 L^2} \sigma_{xx}(L/2, -h/2) \quad , \quad \bar{\sigma}_{xz} = \frac{hb}{p_0 L} \sigma_{xz}(0,0)
$$

(20)

calculated percentage (%) differences compared to the elasticity solution are presented in Table 3. As seen in this table, the finite element formulation for the lamination and loading state exhibits consistent convergence. It is observed that as the beam span-to thickness ratio increases, the results obtained with the proposed method agree better with the elasticity solution. The convergence of the transverse shear stress values is slower compared to deflection and axial stress components, except for the thick beam ($\rho = 5$) example. However, for the ratios $\rho = 5$, $\rho = 10$, and $\rho = 20$, it is observed that the results obtained from this study show a closer agreement with the elasticity solution compared to the results obtained from the finite element solution based on the third order theory.

In Table 4, the displacement and stress components of a uniformly loaded simply supported beam with symmetric [0/90/0] and antisymmetric [0/90] layouts are given in nondimensional

forms according to Equation (21). In this example, a comparison has been made with the analytical solution that Zenkour [21] obtained according to the simple higher order theory. In addition, only the deflection values are compared with Khdeir and Reddy's analytical results. In this problem, it should be noted that the transverse shear stress (σ_{xz}) values presented in Table 4 are calculated over the constitutive relations, instead of equilibrium equations. The handling of the relevant problem by Zenkour [21] in this way has led to this necessity. As seen in Table 4, the proposed mixed finite element solution exhibits a stable convergence behavior. A high level of agreement has been achieved between the analytical results with the mixed finite element solutions for all presented beam span-to-thickness ratios. As can be clearly followed from Table 4, it has been determined that the axial normal stress (σ_{xx}) values converge faster than the other parameters. It can be seen that the results obtained even with the very loose element mesh ($n_e = 10$) coincide well enough with the analytical result.

Table 3 - Comparison of the analysis results of symmetrical laminated, simply supported and uniformly loaded composites with the elasticity solution (percent difference) (Material 2)

Theory	$\rho=5$				$\rho=10$			
	$\overline{w}$	$\overline{\sigma}_{xx}$	$\overline{\sigma}_{xx}^{*}$	$\overline{\sigma}_{xz}$	$\overline{w}$	$\overline{\sigma}_{xx}$	$\overline{\sigma}_{xx}^{*}$	$\overline{\sigma}_{xz}$
MHBT ($n_e = 10$)	5.25	5.84	4.87	3.55	3.31	1.78	1.48	5.64
MHBT ($n_e = 20$)	4.72	5.72	4.75	1.62	2.75	1.74	1.44	1.65
MHBT ($n_e = 30$)	4.63	5.73	4.76	1.83	2.65	1.74	1.44	0.90
MHBT ($n_e = 40$)	4.60	5.73	4.76	2.17	2.61	1.74	1.44	0.76
Kapuria et al.	4.6	5.7	4.8	4.3	2.6	1.7	1.4	1.8
Pagano	2.6748	1.0711	-1.0602	1.432	1.4343	0.9059	-0.9031	8.748
Theory	$\rho=20$				$\rho=100$			
MHBT ($n_e = 10$)	1.65	0.47	0.39	7.51	0.84	0.02	0.02	9.39
MHBT ($n_e = 20$)	1.06	0.46	0.38	2.73	0.24	0.02	0.02	4.37
MHBT ($n_e = 30$)	0.95	0.46	0.38	1.35	0.13	0.02	0.02	2.71
MHBT ($n_e = 40$)	0.91	0.46	0.38	0.80	0.09	0.02	0.02	1.89
Kapuria et al.	0.9	0.5	0.4	0.7	0.0	0.0	0.0	0.0
Pagano	1.1152	0.8641	-0.8635	2.706	1.0123	0.8508	-0.8508	14.62

$$\overline{w} = \frac{10^2 E_2 bh^3}{p_0 L^4} w(L/2, 0) \ , \quad \overline{\sigma}_{xx} = \frac{bh^2}{p_0 L^2} \sigma_{xx}(L/2, h/2) \ , \quad \overline{\sigma}_{xz} = \frac{bh}{p_0 L} \sigma_{xz}(0, 0) \tag{21}$$

Table 4 - Mechanical components of uniformly loaded composite beams with simply supported symmetric and antisymmetric layouts (Material 1)

Layups	Theory	$\rho=5$			$\rho=10$			$\rho=50$		
		$\bar{w}$	$\bar{\sigma}_{xx}$	$\bar{\sigma}_{xz}$	$\bar{w}$	$\bar{\sigma}_{xx}$	$\bar{\sigma}_{xz}$	$\bar{w}$	$\bar{\sigma}_{xx}$	$\bar{\sigma}_{xz}$
[0/90/0]	MHBT ($n_e=10$)	2.3968	-1.0654	0.5330	1.0897	-0.8494	0.5982	0.661	-0.7805	0.6241
	MHBT ($n_e=20$)	2.4098	-1.0670	0.5275	1.0959	-0.8500	0.6138	0.665	-0.7805	0.6577
	MHBT ($n_e=30$)	2.4122	-1.0669	0.5201	1.0970	-0.8500	0.6133	0.666	-0.7805	0.6682
	MHBT ($n_e=40$)	2.4130	-1.0669	0.5150	1.0974	-0.8500	0.6111	0.666	-0.7805	0.6729
	Zenkour	2.4141	-1.0669	0.4057	1.0980	-0.8500	0.4311	0.661	-0.7805	0.4514
	Khdeir and Reddy	2.412			1.096			0.665		
[0/90]	MHBT ($n_e=10$)	4.7487	0.2361	0.2450	3.6675	0.2342	0.2680	3.3179	0.2336	0.2763
	MHBT ($n_e=20$)	4.7761	0.2361	0.2412	3.6894	0.2342	0.2762	3.3379	0.2336	0.2913
	MHBT ($n_e=30$)	4.7811	0.2361	0.2355	3.6934	0.2342	0.2758	3.3417	0.2336	0.2961
	MHBT ($n_e=40$)	4.7829	0.2361	0.2314	3.6948	0.2342	0.2743	3.3430	0.2336	0.2983
	Zenkour	4.7879	0.2362	0.9211	3.6973	0.2343	0.9572	3.3447	0.2336	0.9860
	Khdeir and Reddy	4.777			3.688			3.336		

In Figure 8 (for [0/90/0] layout), the distribution of the transverse shear stress along the cross section of the laminated beam is presented both by calculating in accordance with Hooke's law and by calculating with the equilibrium equations of elasticity. As can be seen from the figure, the transverse shear stress distribution calculated by Hooke's law produces unrealistic results. The reason is that the transverse strain distribution according to the displacement field assumed by the HSDT is continuous throughout the cross section. Therefore, the same
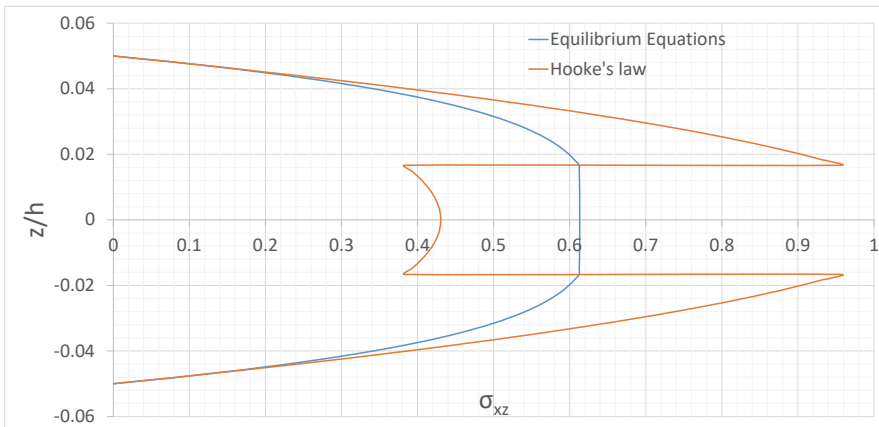

Figure 8 - Uniformly loaded, symmetrical simply supported laminated composite beam with $\rho=20$ ratio and 30 elements (Material 1)

strain and the presence of different material constants in the layer interface cause the transverse shear stress distribution to show discontinuity at these points and need to be calculated incorrectly. In Figure 8, the large difference between the transverse shear stresses calculated using Hooke's law and the equilibrium equation method, which provides a more realistic prediction, can be observed.

Using the advantage of the mixed finite element formulation, stress resultants such as shear force and bending moment are obtained directly (Figure 9, 10 and 11). Figure 9 shows the shear force distribution in a uniformly loaded and simply supported laminated composite beam discretized with 30 elements for $\rho = 5,10,50$ ratios. This distribution overlaps on a large part of the beam for different thickness ratios, and shows slight differences near the supports, where the shear force takes its extremum values.
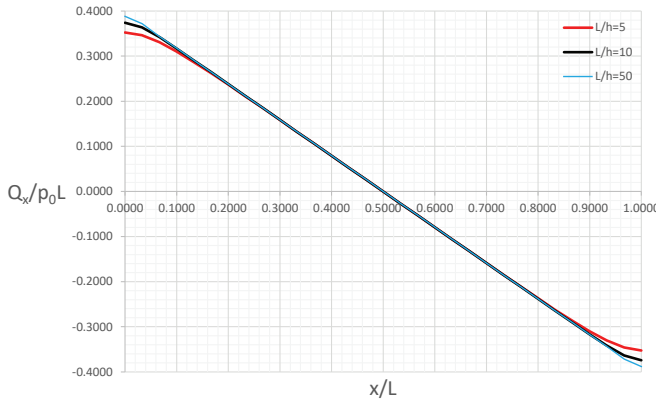

Figure 9 - Shear force distribution of uniformly loaded, symmetrical simply supported laminated composite beam with $\rho = 20$ ratio and 30 elements (Material 1)
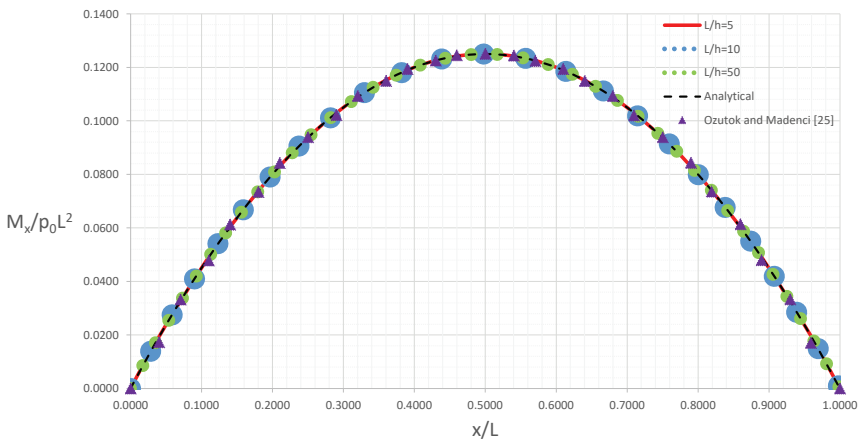

Figure 10 - Moment distribution of uniformly loaded, symmetrical simply supported laminated composite beam (Material 1)

Under the same beam configuration, moment distribution is given for different thickness ratios, and comparison with Ozutok and Madenci [25] can be seen in Figure 10. In this distribution, dimensionless moment values predicted by the MHBT and analytical calculation for all thickness ratios overlap along the beam axis. Therefore, it can be stated that the effect of the transverse shear stresses is not observed in the moment values.
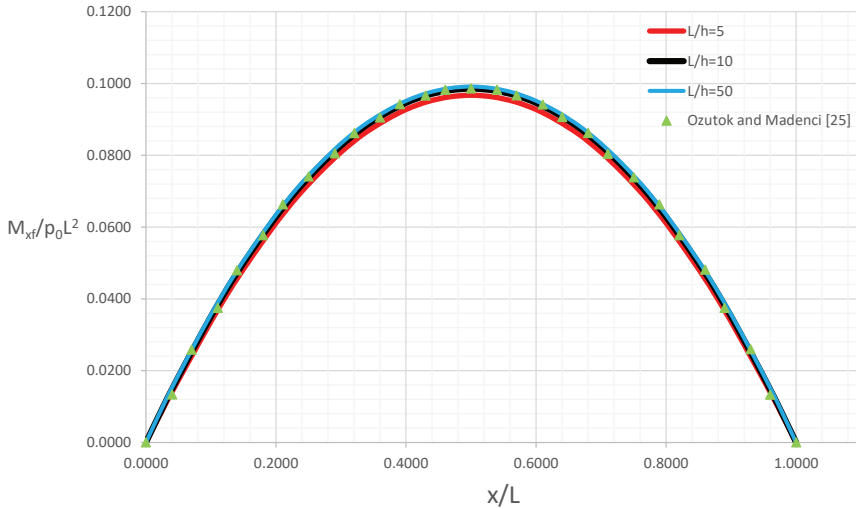

Figure 11 - Higher order Moment distribution of uniformly loaded, symmetrical simply supported laminated composite beam (Material 1)
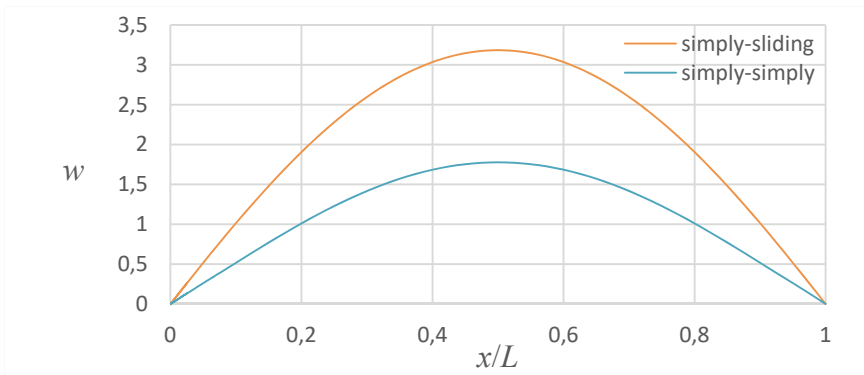

Figure 12 - Deflection (dimensionless) along the beam axis for antisymmetric [0/90] laminated composite beam with $\rho = 20$ ratio

For the same beam, higher order moment distributions are presented for various thickness ratios and also comparison study with Ozutok and Madenci can be followed in Figure 11. Since the higher order moment values along the beam are dependent on the transverse shear

effect, they demonstrate small changes for different thickness ratios. Both for Figure 10 and 11, current study mostly agrees with Ozutok and Madenci [25] $(L/h = 10)$.

In Figure 12, variations of the deflection (nondimensionalized according to Equation (21)) along the beam length for simply-simply supported and simply-sliding supported conditions under uniform loading are displayed. For the simply-sliding case, the maximum deflection value becomes 1.79 times higher than simply-simply case.
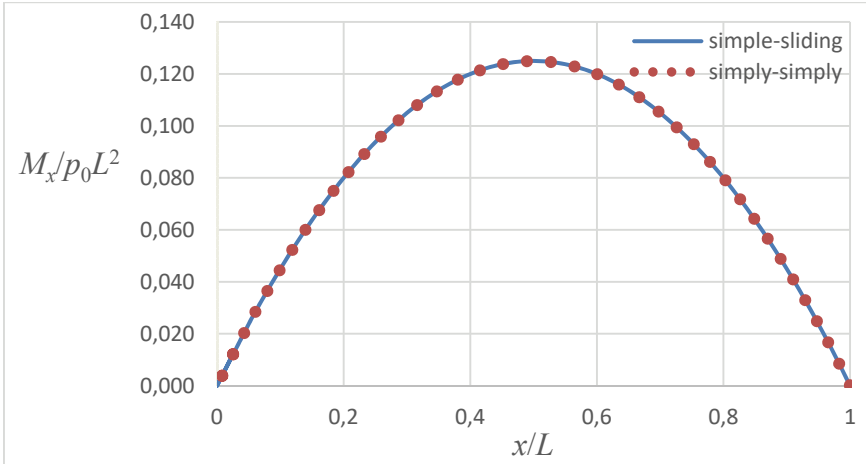

Figure 13 – Moment distribution along the beam axis for antisymmetric [0/90] laminated composite beam with $\rho = 20$ ratio under uniform loading

In Figure 13, the moment distributions along the beam length for simply-simply supported and simply-sliding supported conditions are presented. Both moment distributions overlap similar to the previous example (See Figure 7).

4. CONCLUSION

In this study, displacement and stress distributions of laminated composite beams under various boundary and loading conditions were investigated. For this purpose, a mixed finite element formulation is proposed where governing equations of the laminated beam is obtained by means of a Higher Order Beam Theory. Finite element equations derived using the Hellinger-Reissner variational principle require C_0 continuity. Hence, beam domain is discretized by using linear one-dimensional two-noded elements. As an advantage of the mixed finite element formulation, force and force couple components are calculated directly at the nodes alongside the displacement type field variables. In this way, strain components can be obtained through matrix operations using cross-sectional compliance matrices. In the post-processing, the axial normal stress components are calculated according to Hooke's laws, and the transverse shear stress components are obtained by using the equilibrium equations of the theory of elasticity. In this way the continuity of transverse shear stresses is ensured along the thickness of the laminated beam. Convergence and comparison analyses

were performed in the numerical examples discussed and it was observed that the results were in satisfactory agreement with the exact solutions obtained from the theory of elasticity, analytical solutions and finite element solutions. The effect of extension-bending coupling is demonstrated through some numerical results and it is observed that deflection values are significantly influenced when this coupling takes place. It has been observed that the results are compatible with many advanced finite element solutions that stand out in the literature and can produce even better results in some cases, especially in stress calculations. It is thought that the proposed formulation offers the opportunity to be developed for many types of analysis in the future, and to be adjusted for various problems.

Symbols

$\delta \Pi_{HR}$: First variation of the functional

$\boldsymbol{\varepsilon}^{\mathbf{u}}$: Strain vector in terms of displacement components

$\boldsymbol{\varepsilon}^{\sigma}$: Strain vector in terms of the stress components

$\boldsymbol{\sigma}^{\sigma}$: Stress vector

δ : Variational operator

$\hat{\mathbf{t}}$: Traction vector

Γ : Boundary of the structure

E_1, E_2 : Young's moduli

v_{ij} : Poison's ratio

G_{α} : Shear moduli ($\alpha = 23, 31, 12$)

$f(z)$: Shear functions

h : Thickness

z : Any coordinate along the thickness

$\theta_x(x)$: Shear rotation about y axis

$\sigma_{xx}^{(k)}$: In-plane stress component at k^{th} layer

$\sigma_{xz}^{(k)}$: Transverse shear stress component at k^{th} layer

N_{xx} : In-plane force resultant of stress components

M_{xx} : Resultant moment of stress components

M_{xx}^{f} : Resultant higher order moment of stress components

Q_{xz}	: Resultants of transverse shear stress components
b	: Beam width
N	: Total number of laminates
P	: Stress resultants
$\mathbf{e^u}$	: Strain measures in terms of kinematical variables
E	: Section stiffness matrix
$\mathbf{e^P}$	: Strain measures in terms of stress resultants
p	: Applied load vector
L	: Beam length
K	: System matrix
F	: External force vector
X	: Unknown vector

Acknowledgements

References

[1] V.V. Vasiliev, E.V. Morozov, Advanced Mechanics of Composite Materials and Structural Elements, Elsevier, London, UNITED KINGDOM, 2013. http://ebookcentral.proquest.com/lib/itup/detail.action?docID=1221537 (accessed April 9, 2021).

[2] İ. Çömez, U.N. Aribas, A. Kutlu, M.H. Omurtag, An Exact Elasticity Solution for Monoclinic Functionally Graded Beams, Arab J Sci Eng. 46 (2021) 5135–5155. https://doi.org/10.1007/s13369-021-05434-9.

[3] M. Dorduncu, Peridynamic modeling of delaminations in laminated composite beams using refined zigzag theory, Theoretical and Applied Fracture Mechanics. 112 (2021) 102832. https://doi.org/10.1016/j.tafmec.2020.102832.

[4] M. Dorduncu, Stress analysis of laminated composite beams using refined zigzag theory and peridynamic differential operator, Composite Structures. 218 (2019) 193–203. https://doi.org/10.1016/j.compstruct.2019.03.035.

[5] L. Euler, Methodus inveniendi lineas curvas maximi minimive proprietate gaudentes, apud Marcum-Michaelem Bousquet, 1744.

[6] J. Bernoulli, Curvatura laminae elasticae, Acta Eruditorum Lipsiae. 1694 (1964) 262–276.

[7] B.A. Boley, On the Accuracy of the Bernoulli-Euler Theory for Beams of Variable Section, Journal of Applied Mechanics. 30 (1963) 373–378. https://doi.org/10.1115/1.3636564.

[8] A.H. Modaress-Aval, F. Bakhtiari-Nejad, E.H. Dowell, H. Shahverdi, H. Rostami, D.A. Peters, Aeroelastic analysis of cantilever plates using Peters' aerodynamic model, and the influence of choosing beam or plate theories as the structural model, Journal of Fluids and Structures. 96 (2020) 103010. https://doi.org/10.1016/j.jfluidstructs.2020.103010.

[9] S.P. Timoshenko, LXVI. On the correction for shear of the differential equation for transverse vibrations of prismatic bars, (1921) 3.

[10] W. Wagner, F. Gruttmann, A displacement method for the analysis of flexural shear stresses in thin-walled isotropic composite beams, Computers & Structures. 80 (2002) 1843–1851. https://doi.org/10.1016/S0045-7949(02)00223-7.

[11] U. Lee, I. Jang, Spectral element model for axially loaded bending–shear–torsion coupled composite Timoshenko beams, Composite Structures. 92 (2010) 2860–2870. https://doi.org/10.1016/j.compstruct.2010.04.012.

[12] J.N. Reddy, A simple higher-order theory for laminated composite plates, Journal of Applied Mechanics. 51 (1984) 745–752. https://doi.org/10.1115/1.3167719.

[13] E. Reissner, On transverse bending of plates, including the effect of transverse shear deformation, International Journal of Solids and Structures. 11 (1974) 569–573.

[14] K.P. Soldatos, A transverse shear deformation theory for homogeneous monoclinic plates, Acta Mechanica. 94 (1992) 195–220. https://doi.org/10.1007/BF01176650.

[15] A.J.M. Ferreira, C.M.C. Roque, P.A.L.S. Martins, Radial basis functions and higher-order shear deformation theories in the analysis of laminated composite beams and plates, Composite Structures. 66 (2004) 287–293. https://doi.org/10.1016/j.compstruct.2004.04.050.

[16] M.V.V.S. Murthy, D. Roy Mahapatra, K. Badarinarayana, S. Gopalakrishnan, A refined higher order finite element for asymmetric composite beams, Composite Structures. 67 (2005) 27–35. https://doi.org/10.1016/j.compstruct.2004.01.005.

[17] E. Madenci, Yüksek Mertebe Kayma Deformasyon Teorisine Dayali Çapraz Tabakali Kompozit Plaklarin Karisik Sonlu Eleman Yöntemi İle Analizi, Selcuk Universitesi, 2016.

[18] K. Chandrashekhara, K.M. Bangera, Free vibration of composite beams using a refined shear flexible beam element, Computers & Structures. 43 (1992) 719–727. https://doi.org/10.1016/0045-7949(92)90514-Z.

[19] D.K. Maiti, P.K. Sinha, Bending and free vibration analysis of shear deformable laminated composite beams by finite element method, Composite Structures. 29 (1994) 421–431.

[20] S. Xiaoping, S. Liangxin, An improved simple higher-order theory for laminated composite plates, Computers & Structures. 50 (1994) 231–236. https://doi.org/10.1016/0045-7949(94)90298-4.

[21] A.M. Zenkour, Transverse shear and normal deformation theory for bending analysis of laminated and sandwich elastic beams, Mech. of Adv. Mat. & Structures. 6 (1999) 267–283. https://doi.org/10.1080/107594199305566.

[22] H. Matsunaga, Vibration and buckling of multilayered composite beams according to higher order deformation theories, Journal of Sound and Vibration. 246 (2001) 47–62. https://doi.org/10.1006/jsvi.2000.3627.

[23] P. Subramanian, Dynamic analysis of laminated composite beams using higher order theories and finite elements, Composite Structures. 73 (2006) 342–353. https://doi.org/10.1016/j.compstruct.2005.02.002.

[24] W. Zhen, C. Wanji, An assessment of several displacement-based theories for the vibration and stability analysis of laminated composite and sandwich beams, Composite Structures. 84 (2008) 337–349. https://doi.org/10.1016/j.compstruct.2007.10.005.

[25] A. Ozutok, E. Madenci, Static analysis of laminated composite beams based on higher-order shear deformation theory by using mixed-type finite element method, Int. J. Mech. Sci. 130 (2017) 234–243. https://doi.org/10.1016/j.ijmecsci.2017.06.013.

[26] A. Kutlu, M. Dorduncu, T. Rabczuk, A novel mixed finite element formulation based on the refined zigzag theory for the stress analysis of laminated composite plates, Composite Structures. 267 (2021) 113886. https://doi.org/10.1016/j.compstruct.2021.113886.

[27] A. Kutlu, Mixed finite element formulation for bending of laminated beams using the refined zigzag theory, Proceedings of the Institution of Mechanical Engineers, Part L: Journal of Materials: Design and Applications. 235 (2021) 1712–1722. https://doi.org/10.1177/14644207211018839.

[28] A. Kutlu, G. Meschke, M.H. Omurtag, A new mixed finite-element approach for the elastoplastic analysis of Mindlin plates, J Eng Math. 99 (2016) 137–155. https://doi.org/10.1007/s10665-015-9825-7.

[29] U.N. Aribas, M. Ermis, N. Eratli, M.H. Omurtag, The static and dynamic analyses of warping included composite exact conical helix by mixed FEM | Elsevier Enhanced Reader, Composites Part B: Engineering. 160 (2019) 285–297. https://doi.org/10.1016/j.compositesb.2018.10.018.

[30] U.N. Aribas, M. Ermis, A. Kutlu, N. Eratli, M.H. Omurtag, Forced vibration analysis of composite-geometrically exact elliptical cone helices via mixed FEM, Mechanics of Advanced Materials and Structures. (2020) 1–19. https://doi.org/10.1080/15376494.2020.1824048.

[31] U.N. Aribas, M. Ermis, M.H. Omurtag, The static and stress analyses of axially functionally graded exact super-elliptical beams via mixed FEM, Arch Appl Mech. 91 (2021) 4783–4796. https://doi.org/10.1007/s00419-021-02033-w.

[32] D. Shao, S. Hu, Q. Wang, F. Pang, Free vibration of refined higher-order shear deformation composite laminated beams with general boundary conditions, Composites Part B: Engineering. 108 (2017) 75–90. https://doi.org/10.1016/j.compositesb.2016.09.093.

[33] A.S. Sayyad, Y.M. Ghugal, Bending, buckling and free vibration of laminated composite and sandwich beams: A critical review of literature, Composite Structures. 171 (2017) 486–504. https://doi.org/10.1016/j.compstruct.2017.03.053.

[34] Y. Bab, A. Kutlu, Mixed finite element formulation based on higher order theory for stress calculation of laminated composite beams, in: Proceedings 22. National Mechanics Congress, Adana, Turkey, September 06-10.

[35] P. Shi, C. Dong, F. Sun, W. Liu, Q. Hu, A new higher order shear deformation theory for static, vibration and buckling responses of laminated plates with the isogeometric analysis, Composite Structures. 204 (2018) 342–358. https://doi.org/10.1016/j.compstruct.2018.07.080.

[36] R.M. Jones, Mechanics of composite materials, CRC Press, 1999.

[37] E. Hellinger, Die Allgemeinen Ansätze der Mechanik der Kontinua, in: F. Klein, Conr. Müller (Eds.), Mechanik, Vieweg+Teubner Verlag, Wiesbaden, 1907: pp. 601–694. https://doi.org/10.1007/978-3-663-16028-1_9.

[38] E. Reissner, On a Variational Theorem in Elasticity, Journal of Mathematics and Physics. 29 (1950) 90–95. https://doi.org/10.1002/sapm195029190.

[39] N.J. Pagano, Exact solutions for rectangular bidirectional composites and sandwich plates, (n.d.) 15.

[40] K.A. Hasim, Isogeometric static analysis of laminated composite plane beams by using refined zigzag theory, Composite Structures. 186 (2018) 365–374. https://doi.org/10.1016/j.compstruct.2017.12.033.

[41] P. Vidal, O. Polit, A sine finite element using a zig-zag function for the analysis of laminated composite beams, Composites Part B: Engineering. 42 (2011) 1671–1682. https://doi.org/10.1016/j.compositesb.2011.03.012.

[42] A.A. Khdeir, J.N. Reddy, An exact solution for the bending of thin and thick cross-ply laminated beams, Composite Structures. 37 (1997) 195–203.

[43] S. Kapuria, P.C. Dumir, N.K. Jain, Assessment of zigzag theory for static loading, buckling, free and forced response of composite and sandwich beams, Composite Structures. 64 (2004) 317–327. https://doi.org/10.1016/j.compstruct.2003.08.013.